

Numerical Results of Off-Angle Thermal Spray Particle Impact

M. Bussmann, S. Chandra and J. Mostaghimi

Thermal Spray Laboratory, Department of Mechanical and Industrial Engineering
University of Toronto, Toronto, Canada

Abstract

Results of the influence of the spray angle θ on the shape of thermal spray splats are presented. Simulations were run of the fluid dynamics of impact of Ni particles characteristic of both HVOF and DC plasma conditions. Results demonstrate an elongation of the splats as θ decreases, as one would expect, and confirm previous experimental observations [1] that splat area varies little with spray angle. Results also suggest that greater than 90% of material is deposited “downstream” of the point of impact, even for $\theta=45^\circ$.

1. Introduction

One aspect of the thermal spray process which has received little attention until recently is the effect of spray angle θ (see **Fig. 1**) on coating characteristics. Models of particle impact and of coating formation invariably assume that the particle trajectory prior to impact is perpendicular to the substrate surface ($\theta=90^\circ$). However, as the thermal spray process continues to be adapted to new applications, and as coatings are applied onto increasingly complex substrate geometries, the influence of spray angle on coating characteristics merits further consideration.

A few studies have examined the role of the spray angle on coating characteristics. The conclusions may be summarized as follows: (i) the influence of spray angle for $\theta>45^\circ$ is slight [2,3]; (ii) as the spray angle decreases, especially for $\theta<45^\circ$, porosity and roughness increase [2,3], and mechanical characteristics such as hardness, adhesion strength and fracture toughness decrease [3].

While these studies examined coating characteristics, Montavon et al. [1] used image analysis and statistical techniques to examine the shape of individual splats. They introduced several geometric quantities, including an equivalent diameter ED :

$$ED = \sqrt{\frac{4A}{\pi}} \quad (1)$$

and an elongation factor EF , similar to an aspect ratio:

$$EF = \frac{\pi L^2}{4A} \quad (2)$$

(A refers to splat area and L to the longest dimension across the splat, see **Fig. 2**). Results showed that while EF varies continuously with θ , as might be expected, the splat area as characterized by ED varies little.

Kanouff et al. [4] assumed simple models of splat characteristics as input to a model of coating formation, in an attempt to predict surface roughness as a function of θ .

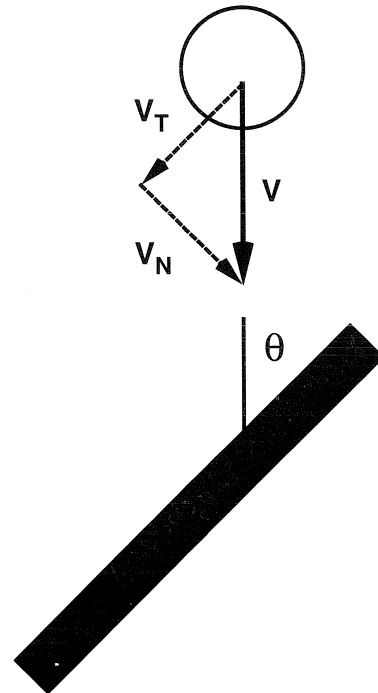


Figure 1. Schematic of off-angle particle impact, including definition of normal (N) and tangential (T) components of impact velocity V , and the impact angle θ .

D_o (μm)	V_o (m/s)	θ ($^\circ$)	V_N (m/s)	Re_N	EF	ED/D_o	f
50	100	90	100	7,500	1.0	4.6	0.5
50	100	45	71	5,300	1.27	4.5	0.07
50	100	30	50	3,700	1.78	4.5	0.01
25	500	90	500	18,600	1.0	6.4	0.5
25	500	45	354	13,200	1.26	5.8	0.05
25	500	30	250	9,300	1.65	5.8	0.01

Table 1. Summary of the results of six simulations of the effect of θ on the impact of a molten Ni particle.

In particular, they proposed an expression for a quantity similar to EF to characterize splat elongation, fitted to the experimental results of Madejski [5], and introduced an additional quantity f to characterize the location of the splat, defined as the fraction of material remaining upstream of the point of impact. For lack of data, they conjectured a simple linear relationship between f and θ :

$$f = \frac{\theta}{180^\circ} \quad (3)$$

The results of their model, utilizing a so-called string method, overpredicted the surface roughness observed experimentally, but correctly predicted the increase of roughness as θ decreased.

The present work was carried out to consolidate some of this data related to splat geometry, utilizing a numerical model to examine the effect of spray angle on particle impact.

2. Method

The numerical model is a three-dimensionalization of RIPPLE [6], a 2D Eulerian fixed-grid fluid dynamics code developed specifically for free surface flows. The model solves the flow equations for convective, viscous and surface tension effects, and tracks fluid deformation during particle impact. The tracking algorithm tracks fluid volume rather than the free surface, and is thus suited to modeling gross fluid deformation. Further details of the model have been presented previously [7].

The model does not account for the solidification of the molten material during impact, so that the results presented here are of the fluid flow only. Also, by contrast to results presented previously [7], the model was configured to inhibit the initiation of particle splashing, in order to focus these results on the bulk deformation of the fluid.

Two sets of simulations were run, corresponding to conditions typical of HVOF and DC plasma spraying,

for the properties of Ni at its melting point. **Table 1** presents a summary of the input conditions. Each set of simulations included runs at $\theta=45^\circ$ and $\theta=30^\circ$, as well the corresponding normal impact ($\theta=90^\circ$). To afford comparison between similar impacts, absolute particle velocity V_o was maintained constant, resulting in variations of the velocity V_N normal to the surface (**Fig. 1**). The Reynolds number, indicative of the inertia of impact, is defined as:

$$Re_N = \frac{\rho V_N D_o}{\mu} \quad (4)$$

Simulations were run to a non-dimensional time $t^*=3$, near the point of maximum fluid spread [8], where t^* is defined as:

$$t^* = \frac{V_N t}{D_o} \quad (5)$$

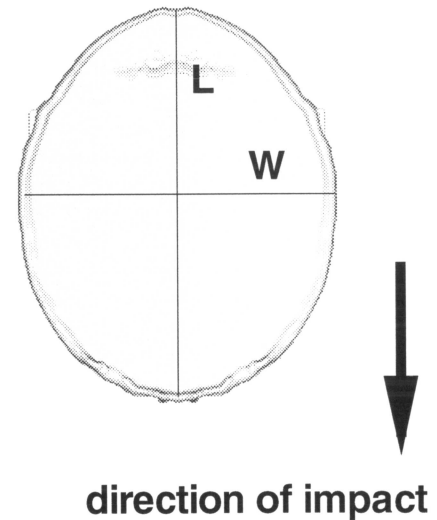


Figure 2. Thermal spray splat resulting from the impact of a $50 \mu\text{m}$ Ni particle at 100 m/s. L and W refer to the maximum length and width of the splat.

3. Results

Table 1 lists the geometric characteristics of the simulated splats, including the EF , the ED normalized by the initial particle diameter (yielding an equivalent spread factor $\xi_{eq}=ED/D_0$), and the fraction f of material remaining above the point of impact. To illustrate the impacts, **Fig. 3** presents a sequence of images of the 30° and 45° impacts of the HVOF particle from the moment of impact to $t^*=3$.

As observed experimentally [1], ξ_{eq} (and thus the splat area A) varies little with θ : for impacts characteristic of a DC plasma spray, ξ_{eq} is nearly constant at 4.5, while the HVOF splat, characterized by a larger Re_N and thus larger ξ_{eq} , shows only a slight decrease in area as θ decreases.

The elongation factor EF , on the other hand, increases as θ decreases, as expected. The values are somewhat smaller than the values reported by Montavon et al. [1], who observed a variation of EF between 1.3 and 2.1 for θ ranging from 90° to 30° . The discrepancy is likely due to several factors: (i) the absence of “real” features such as surface roughness in the model, which might yield asymmetric results even for $\theta=90^\circ$, (ii) the lack of a solidification model. While the values of f listed in **Table 1** reveal that nearly the entire mass of fluid slides beyond the point of impact, it is likely that at least a thin solidified layer of material remains upstream, yielding somewhat larger values of both EF and f . The lack of a solidification model notwithstanding, it would seem that the relationship between f and θ varies more strongly than simply linearly (Eq. 3).

A final note concerns the flow of material as pictured in **Fig. 3**. As the splat advances, fluid accumulates near the bottom of the splat, and finally yields a ragged leading edge as this material jumps beyond the contact line. Particle impact onto a rough surface would likely exaggerate such an effect, and may be an example of the “overspray” described by Kannouf et al. [4].

4. Conclusions

Results have been presented of simulations of off-angle Ni particle impacts characteristic of both HVOF and DC plasma sprays. While splat area remains relatively constant with spray angle, splats do tend to elongate as the angle decreases, in keeping with experimental observations. Results also reveal that greater than 90% of material accumulates “downstream” of the point of impact.

5. References

- [1] Montavon, G., S. Sampath, C.C. Berndt, H. Herman, C.Coddet: Effects of the spray angle on splat morphology during thermal spraying, *Surf. Coat. Technol.* **91** (1997), pp. 107/115.
- [2] Smith, M.F., R.A. Neiser and R.C. Dykhuizen: An investigation of the effects of droplet impact angle in thermal spray deposition, *Proc. 7th NTSC*, Boston, MA (1994), pp. 603/608.
- [3] Leigh, S.H. and C.C. Berndt: Evaluation of off-angle thermal spray, *Surf. Coat. Technol.* **89** (1997), pp. 213/224.
- [4] Kanouff, M.P., R.A. Neiser, Jr. and T.J. Roemer: Surface roughness of thermal spray coatings made with off-normal spray angles, *J. Therm. Spray Technol.* **7** (1998), pp. 219/228.
- [5] Madejski, J.: Solidification of droplets on a cold surface, *Int. J. Heat Mass Transfer* **19** (1976), pp. 1009/1013.
- [6] Kothe, D.B., R.C. Mjolsness and M.D. Torrey, Technical Report LA-12007-MS, LANL (1991).
- [7] Bussmann, M., S.D. Aziz, S. Chandra and J. Mostaghimi: 3D modelling of thermal spray droplet splashing, *Proceedings of the 15th ITSC*, Nice, France (1998), pp. 413/418.
- [8] Pasandideh-Fard, M., Y.M. Qiao, S. Chandra and J. Mostaghimi: Capillary effects during droplet impact on a solid surface, *Phys. Fluids* **8** (1996), p. 650/659.

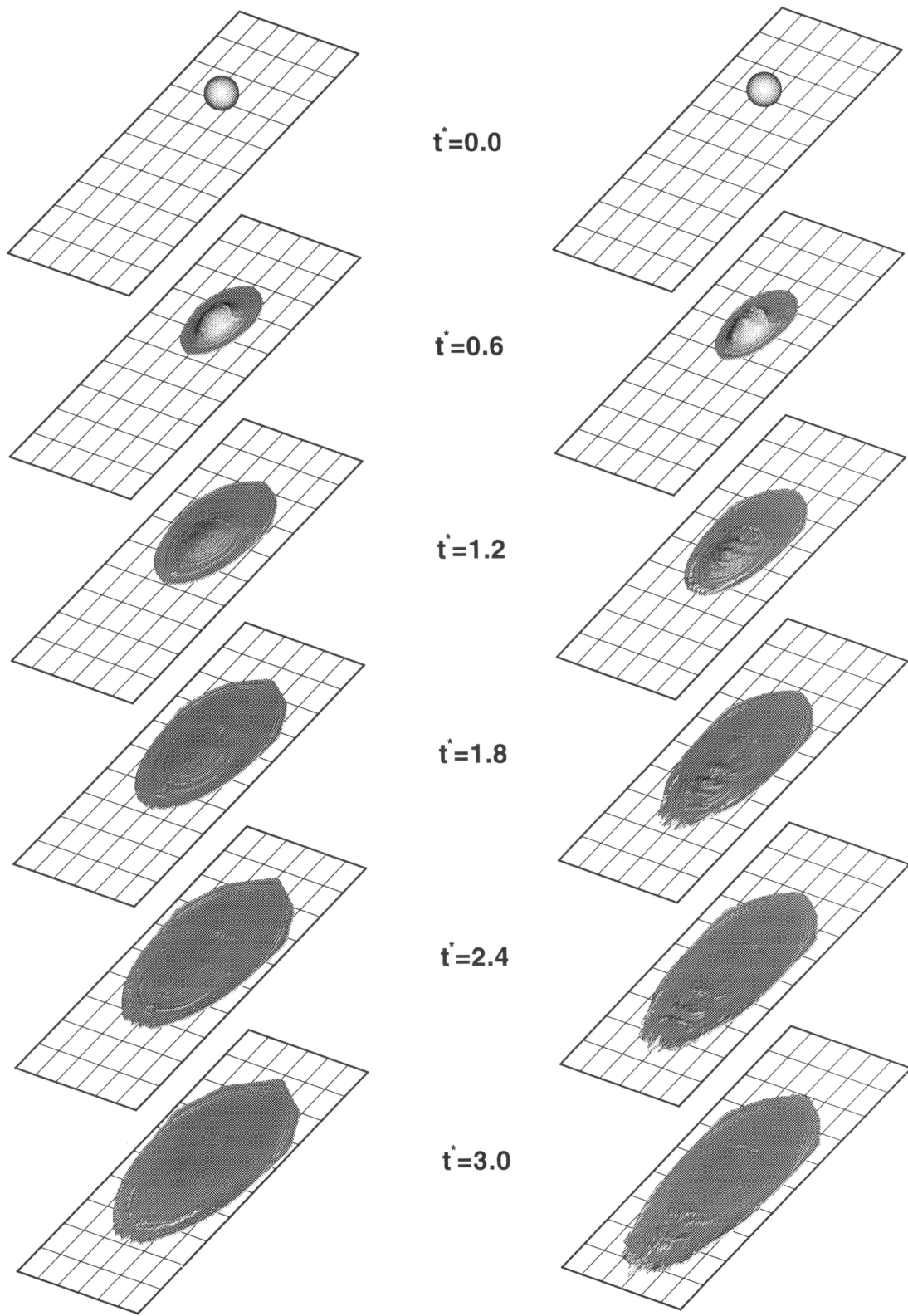


Figure 3. Comparison of the impact of a 25 μm Ni particle at 500 m/s onto a solid surface at $\theta=45^\circ$ (left) and $\theta=30^\circ$ (right).